Modification of near-surface layers of alpha-gallium oxide under irradiation with ultrahigh ion doses

© E.D. Fedorenko[1], A.I. Klevtsov[1], A.I. Titov[1], V.D. Andreeva[1], A.L. Shahmin[1], P.A. Karaseov[1], A.I. Pechnikov[2], V.I. Nikolaev[2]

[1] Peter the Great Saint-Petersburg Polytechnic University,
195251 St. Petersburg, Russia
[2] Ioffe Institute,
194021 St. Petersburg, Russia

E-mail: lizasever69@mail.ru

Received October 3, 2024
Revised October 29, 2024
Accepted November 11, 2024

A detailed study of α-Ga_2O_3 epitaxial layers grown by halide vapor phase epitaxy has been carried out both before and after P and Ta and molecular PF_4 ion bombardment to doses as high as 45 dpa. A wide range of complementary analytical techniques were used: X-ray diffraction, atomic force microscopy, Rutherford backscattering spectrometry in channeling mode and X-ray photoelectron spectroscopy. Completely amorphous layer is formed from the surface to the crystal bulk as a result of irradiation. Monatomic P and Ta ions form thicker amorphous layer than molecular PF_4 ions. Small step appears at the border between virgin and irradiated areas of the sample revealing sample swelling ($\sim$ 7 nm after irradiation to 45 dpa). The root mean square roughness of the α-Ga_2O_3 surface remains approximately unchanged (0.7 to 0.5 nm) after irradiation to a dose up to 45 dpa, regardless of the ion kind. The smoothing of small scale topography (reflecting atomic steps) due to irradiation-induced amorphization of the sub-surface layer is found, whereas the large scale topography remains virtually unchanged. Ion bombardment leads to surface layer decomposition with oxygen loss and partial reduction of gallium to Ga^0 and Ga^+ states.

Keywords: gallium oxide, α-Ga_2O_3, ion bombardment, high-dose irradiation, modification of sub-surface layers, ion radiation effects, Surface topography, structural defects, X-ray photoelectron spectroscopy, AFM.

DOI: 10.61011/SC.2024.09.59921.7126

1. Introduction

Semiconductors necessary for the creation of a new generation of powerful electronic devices and optoelectronics have been intensively searched and studied in recent years. SiC and GaN have been gradually replacing silicon, but technological difficulties limit the possibilities of sufficiently cheap mass production of power devices based on these two materials. A group of oxide semiconductors are among the other main candidates. Gallium oxide Ga_2O_3 attracts great interest among them. It has the following advantages as a base material for semiconductor devices: wide band gap (4.5–5.3 eV for different phases), high breakdown voltage values ($\sim$ 8 MV/cm) [1–3]. There are five different polymorphic modifications of Ga_2O_3: monoclinic (β-Ga_2O_3), rhombohedral (α), defective spinel (γ), cubic (δ) or orthorhombic (ε) structures. β-polymorph is the only thermostable form under normal conditions among them. At the same time, the polymorph α-Ga_2O_3 has a higher band gap (5.3 eV) and, as a result, may have an even greater breakdown voltage [4]. Gallium oxide has the potential to be used in practical applications such as UV detection, photocatalysis, flat panel displays, UV filters, gas sensors, and optoelectronic devices. It is assumed that many of the devices based on Ga_2O_3 will work in radiation-harsh conditions, for example, in military systems, ozone layer monitoring, in aviation and space systems, robotic inspection systems used near reactor cores, etc.,where they can be exposed to energetic particles. In addition, the nanoparticles Ga_2O_3 can be used as multifunctional drug carriers, and their luminescence can be used to monitor the distribution of drugs inside cells [5].

It is necessary to study the properties and characteristics of gallium oxide and ways to modify them for development of a technology for creating instrument structures. The ion irradiation is one of the main methods used to selectively change properties in the manufacture of semiconductor devices, including the creation of electrically insulating areas, the introduction of alloying impurities, etc. However, accelerated ion irradiation is accompanied by the formation of radiation damage in the target. Impinged ions collide with atoms in the lattice, which knocks them out of their regular positions, and so-called displacement cascades are formed, consisting of vacancies and interstitial atoms [6]. The formed point defects diffuse, recombine, and interact with each other and various sinks in the target to form stable damage to the crystal lattice. The local concentration of point defects formed in the cascade region affects the course of ion-stimulated defect formation [7–10]. The local density of displacement cascades created in the target by inhibited ions is one of the important parameters that significantly affect the effectiveness of the formation of stable radiation defects. It is convenient to study the effects associated with an increase in cascade density by comparing the accumulation

of damage formed by irradiation with molecular and atomic ions [7,8].

It was previously shown that structural damage in α-Ga_2O_3 irradiated with small doses is bimodal in nature [9–12]. Two pronounced maxima are found on the spectra, corresponding to the appearance of a strongly disordered layer just under the surface of the target (the surface maximum of defects) and the formation of a disordered region in the bulk (the bulk maximum of defects). The study of the dynamics of radiation defects [11] in single crystals α-Ga_2O_3 implanted with Ni ions with an energy of 400 keV, showed that, unlike βpolymorph, intrinsic defects in α-Ga_2O_3 are highly mobile even at room temperature. Thus, the structural damage accumulates in two different areas at the surface and in the crystal bulk. The results obtained at low doses indicate that the concentration of damage to the structure of polymorphs α- and β-Ga_2O_3 is higher than that of GaN. At the same time, the rate of accumulation of defects both in the crystal volume and on the surface of β-Ga_2O_3 is approximately an order of magnitude higher than that of α-Ga_2O_3 and GaN. This indicates that β-Ga_2O_3 is more susceptible to damage in case of an ion bombardment [12]. Significant changes of surface roughness and thickness of the irradiated layers were observed in case of irradiation by GaN with very high doses (15−60 dpa). In this case, it turned out that the course of these processes significantly depends on the density of the displacement cascades. A swelling (swelling of the irradiated material) is observed in case of irradiation with ions forming cascades of low density, and on the contrary, a decrease of the layer thickness is observed with the increase of the density [8]. Also, the formation of surface nanostructures and nitrogen-filled nanobubbles in the near-surface layer of [8,13] was found in gallium nitride, as well as extremely large swelling of the irradiated target region, accompanied by decomposition of the irradiated layer with loss of nitrogen [14].

Of course, it is not necessary to use such large doses to implant impurity atoms in order to create doped regions in semiconductor devices. However, the results of such studies and the resulting effects may be of both purely physical and applied interest. Indeed, high ion doses are used for target sputtering during the secondary ion mass spectrometry studies [15] and irradiation with focused ion beams. The effects described above result in the distortions of the obtained SIMS data (this was experimentally shown for GaN [16]) and during fabrication of cross sections for electron microscopy [17].

Studies of the effects of ion irradiation on gallium oxide are in their infancy. It is impossible to predict the effect of ion irradiation on a complex system in advance, since the processes occurring in this case are significantly nonequilibrium. While a progress has been made for β-Ga_2O_3 in experimental studies on this topic due to the higher thermal stability of this polytype [18], the information about the effects of ion irradiation on the properties of α-phases is extremely limited, and the effects of such high doses have not been studied at all.

We study the effect of bombardment by accelerated molecular (PF_4) and atomic (P, Ta) ions with doses of 30 and 45 dpa in this paper (here dpa is a unit of dose measurement; Displacements per Atom) on the properties of α-Ga_2O_3.

2. Experiment procedure

Epitaxial films of α-Ga_2O_3 with a corundum structure were studied in this paper. $\sim 2\,\mu$m thick layers of α-Ga_2O_3 were grown on the c-planes of a sapphire substrate by chloride gas-phase epitaxy at a temperature of 500°C in LLC „Perfect Crystals“ [19]. The resulting films were transparent, mirror-smooth, and crack-free. The crystallographic structure of the initial samples was studied by X-ray diffraction analysis (XRD) using Θ-2Θ diffractometer D8 Advance Bruker with Bragg-Brentano focusing.

The samples were irradiated with P^+, PF_4^+, and Ta^+ ions on a 500 kV HVEE implanter. Each implantation was performed at room temperature at an angle of 7° from the direction of [0001] to avoid channeling and related effects. Irradiation conditions were chosen to fulfill the requitrements set in ref. [20] for meaningful comparison of the results of bombardment with P, Ta and PF_4. The following parameters should be kept unchanged in order to achieve this: the ion dose expressed per unit atomic mass, the ion energy expressed in dpa — the average number of displacements per target atom at the depth of the maximum elastic energy loss of bombarding ions, as well as the current density in dpa/s. The dpa values were calculated based on the ratio $\mathrm{dpa} = (n_v\Phi)n_{\mathrm{at}}$, where n_v — the average total concentration of vacancies generated by one ion in both sublattices at the depth of the maximum elastic losses (calculated in a pair collision model using the TRIM software [21], Φ — ion fluence in cm^{-2}, n_{at} — atomic concentration α-Ga_2O_3, equal to $1.03 \cdot 10^{23}\,\mathrm{cm}^{-3}$. If these conditions are met, the only difference between irradiation with molecular and atomic ions will be the different density of the collision cascades. The depth distribution of the point defect concentration and the rate of their generation will be the same for all types of ions. All irradiation parameters used in our experiments are listed in the table.

The degree of disordering of the crystal lattice in the near-surface region of the targets after irradiation was studied by the Rutherford backscattering method in combination with channeling (RBS/C). A beam of He^{++} ions in the direction [0001] with an energy of 0.7 MeV was used, scattered into the detector at an angle of 103° to the direction of incidence of the analyzing beam to increase the depth resolution.

The surface topography was studied by atomic force microscopy (AFM) using „Nano — DST“ microscope from Pacific Nanotechnology. The measurements were performed

Table 1. Ion beam fluences and currents used in Irradiation

Ion and energy, keV	Current density				Dose, $\times 10^{16}$ see^{-2}	
	μA/cm^{-2}		10^{-3} dpa/c			
	30 dpa	45 dpa	30 dpa	45 dpa	30 dpa	45 dpa
P 40	0.242	0.484	2.41	4.82	1.89	2.84
PF_4 140	0.076	0.152	2.41	4.82	0.59	0.89
Ta 150	0.047	0.094	2.41	4.82	0.37	0.55

using a semi-contact method, which made it possible to minimize the impact of the probe on the sample surface with the best resolution of the images obtained. TipsNano NSG01 probe was used, the radius of the needle tip was 10 nm, and the stiffness coefficient was 1.45−15.1 nm. The images were processed in Gwyddion software package.

The structure of chemical bonds was analyzed using X-ray photoelectron spectroscopy (XPS) at the facility NanoFab-25 produced by HT-MDT using MgK_αC radiation at 1253.6 eV and the SPECS FG20 flood gun at 10 eV and 5 μA. The energy scale of the ESCA spectrometer was calibrated along the golden line $4f/7/2$, for which the binding energy was set to 84.00 eV. The charge effect was taken into account along the carbon line corresponding to C−H bonds with an energy of 285 eV. A good agreement between the position of the lines of the remaining elements in the sample and their expected chemical state was observed. The number of signal accumulation scans is ≥ 25. In addition to the survey spectra, signals were measured in detail in the energy range corresponding to the positions of the maxima of oxygen O1s and gallium Ga2$p_{3/2}$ atoms. The spectra of individual lines were recorded with a step of 0.1 eV and a transmission energy of 20 eV in the analyzer. The base vacuum was $\sim 2 \cdot 10^{-9}$ Torr.

3. Experimental results

3.1. X-ray diffraction

The initial samples are an epitaxial film α-Ga_2O_3 grown on the surface of a sapphire substrate. The crystal structure was studied using X-ray diffraction analysis. Figure 1 shows a part of the X-ray diffraction pattern of the studied film α-Ga_2O_3 in the range of angles 2θ from 30 to 50°.

The spectrum shows the dominant peak at $2\theta = 40.7°$, which corresponds to the reflection from the system of planes (0006) α-Ga_2O_3. The second largest maximum, near 42.1°, corresponds to the diffraction reflection (0006) from the sapphire substrate. In addition to the main maxima reflecting the presence of alpha aluminum oxides (substrate) and gallium (film), a small peak is also visible in the region of 38.9°, presumably a reflection $(\bar{4}02)$ of ε-phase, indicating the presence of its small inclusions. The observed peak asymmetry is explained by the presence of a doublet in the Cu-K_α line, which resolves by diffraction on the

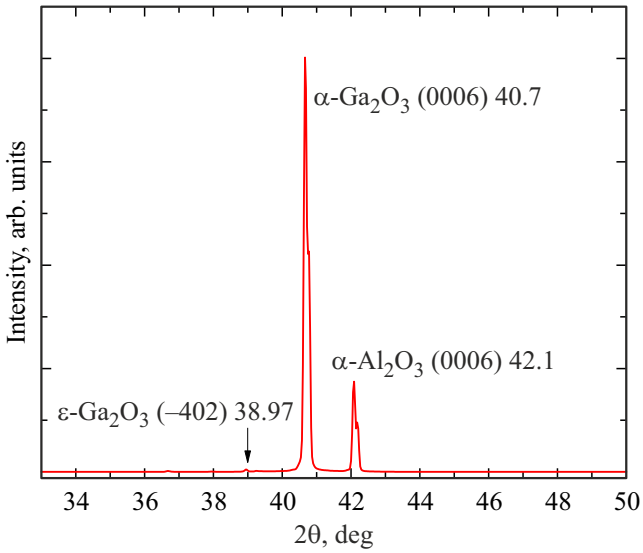

Figure 1. Θ-2Θ X-ray scan of the original sample of α-Ga_2O_3.

studied sample. The X-ray image confirms that the grown film mainly consists of a α-phase. The broadening of the lines is also not observed, so it can be concluded that there are practically no elastic stresses in the film. So, the initial sample is an epitaxial film of α-Ga_2O_3 with a small inclusion of other phases.

3.2. Surface topography

The images of the surface topography of the samples were obtained using atomic force microscopy. A typical relief of the initial surface α-Ga_2O_3 is shown in Figure 2, *a*. Similar patterns have been observed in other studies [22,23]. The morphology of the film surface on the surface of the sapphire substrate consists of elements of two scales: a small ragged and larger tubercles (see Figure 2, *a*). The inserts in Figure 2 show the profile line of atomic steps drawn along the relief of one of the tubercles. The formation of a hilly structure is attributable to the increase of the thickness of the grown film during deposition due to the attachment of part of the Ga and O adatoms to the steps, which initially have approximately the same height. As a result, the flat structure is destabilized, which leads to a pile of steps and the appearance of a larger-scale relief [24].

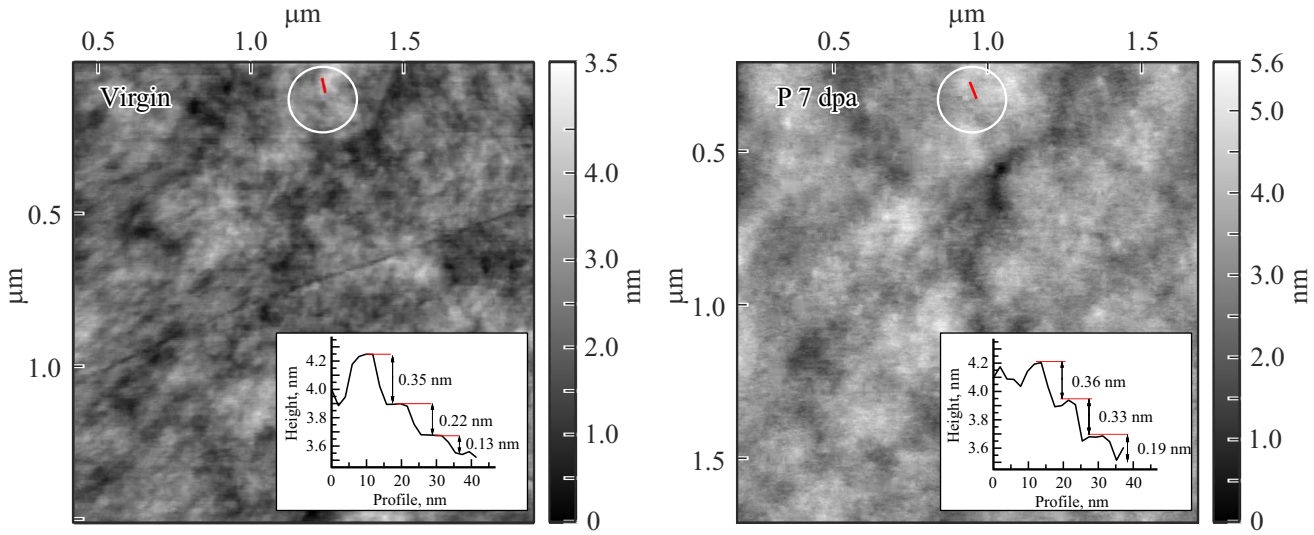

Figure 2. AFM images of the surface of gallium oxide before and after irradiation to a dose of 7 dpa.

For the same reason, the steps seen in the box in Figure 2 have different heights. In our case, the minimum height of the step in the AFM image is approximately ~ 0.11 nm, which coincides with 1/10 of the height value along the direction [0001] of the unit cell α-Ga_2O_3. [25]. For a more detailed study of the morphology details, the frequency spectrum present on AFM scans was decomposed into lower and higher components. The results are listed in Table 2. The decomposition was performed using a two-dimensional Fourier transform in the Gwyddion software package. The selection of the applied mask during frequency separation took place in such a way as to separate both types of relief from each other as much as possible. The resulting images clearly show a fairly smooth surface of the original area, which has two scales of characteristic dimensions. As mentioned above, a small-scale relief is characterized by a structure with ragged ledges corresponding to atomic steps, while a large-scale one occurs due to spatial instabilities of growth, leading to an uneven accumulation of steps.

Ion bombardment leads to a change of topography and can also cause a change in the thickness of the irradiated layer. In our case, irradiation with P ions with an energy of 40 keV and a dose of 7 dpa has practically no effect on the surface relief (see Figure 2, *b*). Table 2 shows AFM images of the surface of gallium oxide after high-dose irradiation with P, PF_4 and Ta ions with energies of 40, 140 and 150 keV, respectively. It can be seen that the fine relief is significantly smoothed out with an increase of the ion dose, losing its features. Visually, the clarity of the surface morphology disappears, but the outlines of the tubercles forming a large-scale relief remain clearly visible. The comparison of the topography profile of the crystallites of the initial and irradiated regions shows the modification and disappearance of the atomic steps forming the structure of the hill. The crystallite slope consisted mainly of several atomic steps with a height range of

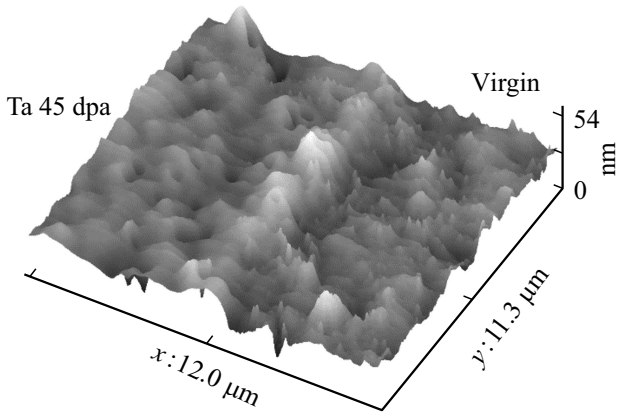

Figure 3. AFM images of a step at the boundary of the irradiated and non-irradiated regions of the gallium oxide surface.

1.1 nm $\pm$ 0.05 nm before the ion bombardment. Relatively smooth and large protrusions are broken into smaller steps with a height range from 0.1 to 0.35 nm,$\pm$,0.05 nm with an increase of the dose up to 45 dpa. The concentration of such protrusions on the same length of the profile section presumably increases and the size decreases. Now the smoothed steps are the main structural element of the ion-irradiated crystallite profile. It should be noted that even with such high-dose irradiation the modification of the relief α-Ga_2O_3 weakly depends on the type of bombarding ion unlike that observed with gallium nitride [8]. The RMS roughness (R_q) of the surface practically does not change in case of exposure to the irradiation (see Table 3). The value of R_q for the initial region was ~ 0.67 nm. The roughness remains ~ 0.70 nm in case of irradiation with a dose of 30 to 45 dpa for lighter ions P, and the roughness slightly decreases on average from 0.64 to 0.59 nm and from 0.60 to 0.48 nm, for heavy ions of PF_4 and Ta, respectively.

Table 2. Two-dimensional Fourier transform. AFM images of large-scale and small-scale surface relief after irradiation by PF_4 ions with a dose of 30 dpa

Virgin	P 30 dpa	PF4 30 dpa	Ta 30 dpa
AFM Image			
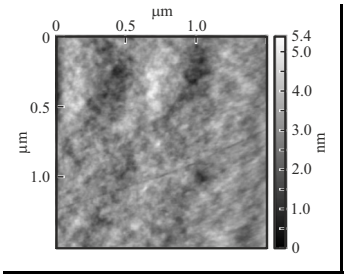	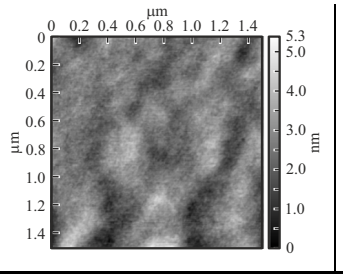	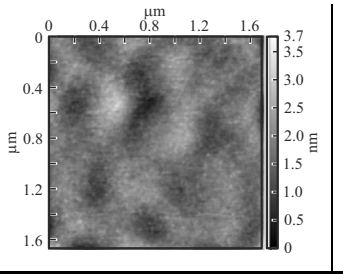	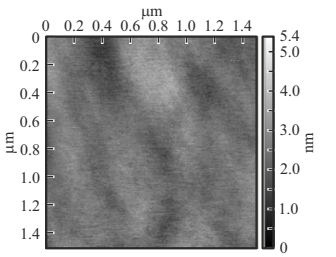
Large scale relief			
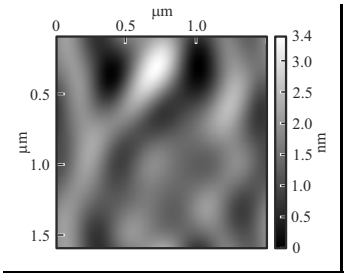	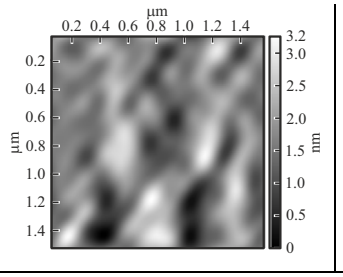	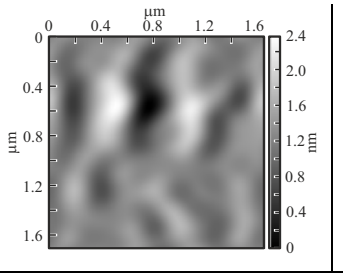	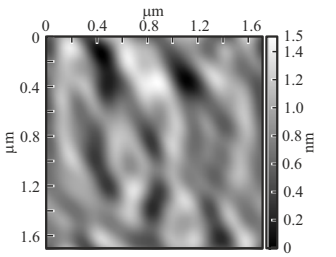
Small scale relief			
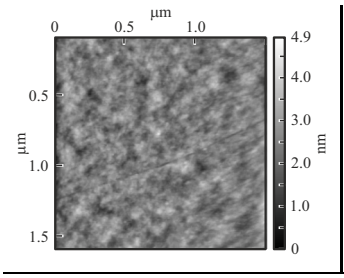	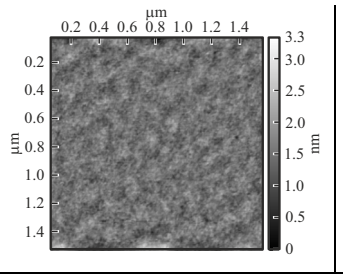	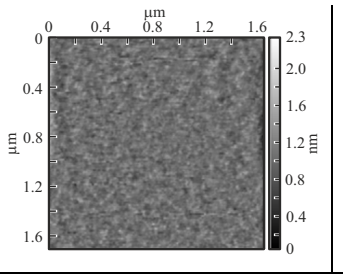	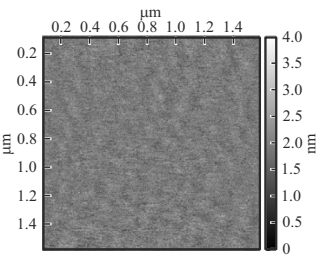
Profile			
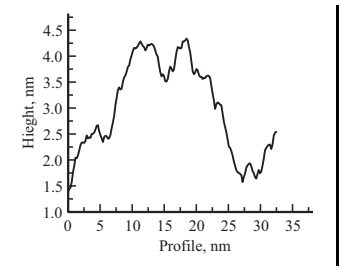	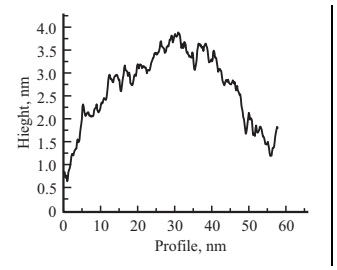	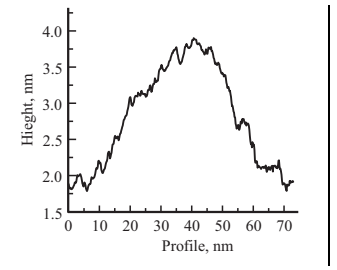	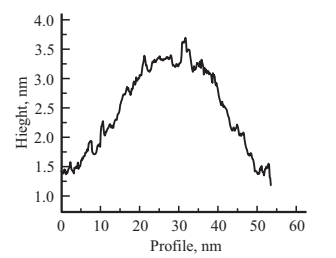

Figure 3 shows a three-dimensional AFM image of the boundary between the irradiated Ta ions and the initial regions of gallium oxide. A small step appears in the images when the dose of all used ions is increased to 45 dpa: the surface on the irradiated side is higher than it was before irradiation. The average step height was 5 nm. In this case, the implantation of molecular and atomic ions leads to a slight swelling of the irradiated area. For the high-dose irradiation used, it is not quite usual that there is no noticeable change in the thickness of the modified layer. The observed effect may be attributable to the following reasons. First, sputtering of the target should be observed in case of irradiation with heavy ions. Table 3 shows the sputtering coefficients calculated using the pair collision model [21] and estimates of the thicknesses of the sputtered layers in case of irradiation with respective ion doses. Sputtering with a molecular ion was taken as the sum of the sputterings produced by its components,

Table 3. Surface parameters and spray parameters

Ion	RMS roughness, nm		Step height, nm		Coefficient of sputtering, at/ion			Thickness of sputtered layer, nm	
	30 dpa	45 dpa	30 dpa	45 dpa	Ga	O	Total	30 dpa	45 dpa
Source	0.67		O						
F				–	1.19	1.95	3.14		
P	0.70	0.73	0	7.5	2.15	3.48	5.63	10.3	15.5
PF_4	0.64	0.59	0	4	3.34	5.43	18.17	10.4	15.6
Ta	0.60	0.48	0	5	6.57	10.71	17.28	6.2	9.2

the synergistic effect was not taken into account. It can be seen that irradiation to a dose of 45 dpa should result in the removal of a layer with a thickness of 10–15 nm from the target surface, depending on the type of ion. On the other hand, the formation of defects in the structure of the crystal lattice can lead to a decrease of the local density, causing swelling. Measurements of the Rutherford backscattering spectra were performed to study the degree of lattice destruction.

3.3. Crystal structure

Irradiation with accelerated ions leads to the appearance of defects in the crystal structure, since when the ions are decelerated, energy is transferred and the atoms of the target are displaced from their places. The formed were studied by using the Rutherford backscattering spectrometry method was used in combination with channeling (RBS/C), where the depth scale can be compared to the energy spectrum of the detected particles. Figure 4 shows the RBS/C spectra before (virgin) and after irradiation of α-Ga_2O_3 with P, PF_4 and Ta ions with a dose of 45 dpa. The distributions of generated vacancies obtained as part of the approximation of paired collisions by the TRIM simulation program are also shown [21]. Unlike the cases of low-dose irradiation [9,10], when the distribution of defects is bimodal (separate peaks corresponding to the formation of two damaged areas are present: near the surface and in the depth of the target) one extended maximum is visible in our case on the channeled spectra of all irradiated samples). This is attributable to the fact that the surface and volume peaks reached their maximum values and became very wide as the radiation dose increased, which led to their fusion. So, the experimental conditions of irradiation are such that the number of point defects created per unit of time per unit volume at the surface of the oxide by ions of each type is the same. However, the number of defects in the subsurface layer formed by ion irradiation depends on the type of bombarding ions as the experiment shows: it is maximal when irradiated with phosphorus ions, minimal when bombarded with molecular ions of PF_4 and has an intermediate value for tantalum ions. The nature of this effect is easily explained if we take into account

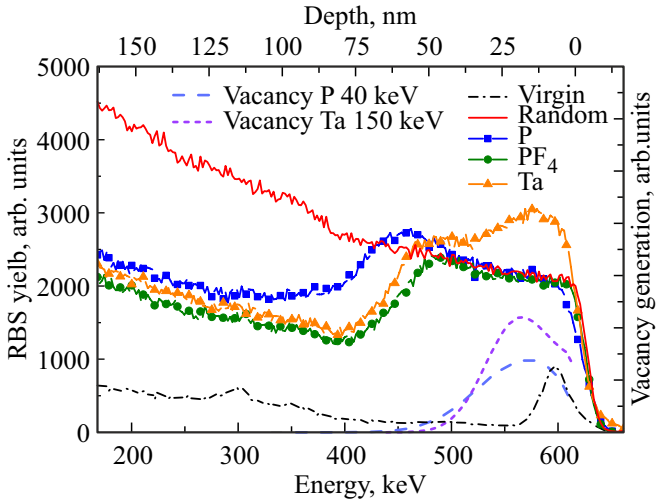

Figure 4. RBS/C spectra from α-Ga_2O_3 samples before and after ion irradiation show the vacancy distributions created in the target by phosphorus and tantalum ions. (A color version of the figure is provided in the online version of the paper).

the differences of the density of the averaged individual cascades [9,20]. Indeed, they „break“ into their components after crossing the target surface by a molecular ion, due to the low bond energy of the atoms in the molecule, moving after that as separate atoms and creating their subcascades [20]. These subcascades overlap before they disperse as long as the penetration depth is low, forming a combined, very dense cascade. Further, each of the subcascades develops independently of the others, creating a concentration of stable disturbances in accordance with its density. This will be mainly the density of the fluorine cascades in the case of the introduction of PF_4 ions. The densest cascades should form in case of bombarding with tantalum ions. Also, „chemical“ stabilization of point defects by embedded phosphorus atoms can lead to an increase of the thickness of the amorphous layer in case of irradiation with P ions. However, this assumption requires further studies.

The spectrum obtained by irradiating the target with tantalum ions also shows that in the depth range from the surface to $\sim$ 37 nm, the probability of backscattering

probing particles is higher than it was in a random direction from the initial sample Ga_2O_3. The inhibition of Ta ions was simulated in the TRIM program to determine the cause of this atypical behavior and their concentration distribution over depth was obtained. Doses of 30 and 45 dpa at a depth of 28 nm correspond to ~ 1.5 and 2.25 at% of tantalum, respectively. These are quite significant values, which may be the reason for the increase in the backscattering signal due to the addition of the intensities of two signals: from gallium atoms located on the target surface and from embedded tantalum atoms located shallow from the surface of the sample of Ga_2O_3. The excess of the „random" signal in the channeled spectrum of phosphorus ions at depths of 50–60 nm is explained similarly.

3.4. X-ray photoelectron spectroscopy

X-ray photoelectron spectroscopy (XPS) studies were performed to study the elemental and chemical state of the disordered layer, which is formed parallel to the surface as a result of its irradiation with molecular and atomic ions. Signals in the energy range corresponding to the main elements were measured in detail in addition to the survey spectra: O1*s* and Ga2$p_{3/2}$. They can be used to judge the structure of chemical bonds in films. Figure 5 shows an overview photoelectron (PE) spectrum of films irradiated with P, PF_4 and Ta ions with a dose of 45 dpa. The intensity values are presented in arbitrary units, and the spectra are shifted vertically relative to each other to simplify perception. A number of peaks are visible, their relation to the main elements was determined according to their energy ranges based on the previously published data [26,27]: O1*s* (530.5–531.5 eV), Ga3*d* (20.2 eV), Ga3*p* (105.8 eV), Ga3*s* (163.4 eV), Ga2$p_{3/2}$ (1118.5 eV) and Ga2$p_{1/2}$ (1145.4 eV). Peaks corresponding to the

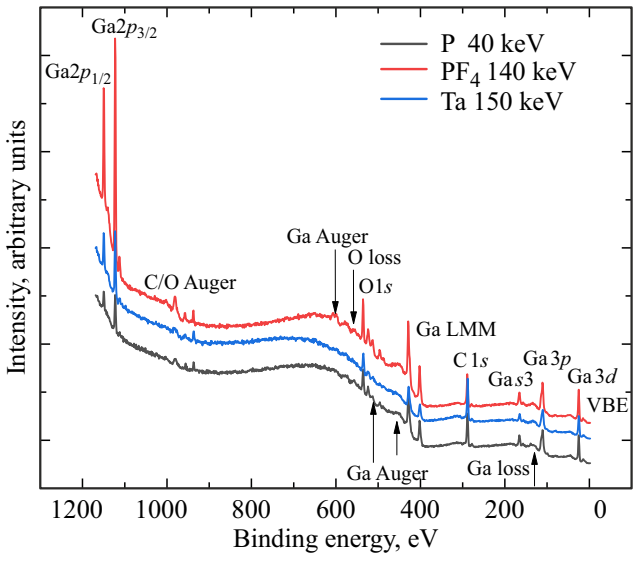

Figure 5. Overview spectra of X-ray photoelectrons of irradiated gallium oxide samples.

Table 4. Relative oxygen content in the subsurface layer of Ga_2O_3

Region	Content of oxygen, %
Virgin	63
P	36
PF_4	15
Ta	21

Auger effect on Ga LMM (402.4 and 408.7 eV) and C/O (937.3, 957.2 and 982.5 eV) atoms and characteristic lines of valence band photoelectrons are also visible. In addition, a small number of carbon atoms (C1*s*, 285 eV) are present on the surface, caused by unintentional contamination during the transfer of samples to the research chamber in air [27]. The surface of the samples was etched with argon ions with an energy of 5 keV for 5 minutes before obtaining detailed XPS spectra for removal of unwanted carbon contamination.

Figures 6 and 7 show detailed XPS spectra of oxygen O1*s* and gallium Ga2$p_{3/2}$ lines obtained from the initial and irradiated samples, respectively. Atoms and chemical bonds were decomposed into components to determine their states. The experimental curves were decomposed in accordance with the parameters found in the literature [26–29] on a line described by a symmetric Gauss-Lorentz function with background approximation by the Shirley method. The width of all lines at half height was ~ 1.6 eV. Let's look at the results in more detail.

O1*s* spectrum obtained from the surface of the initial sample shows the presence of an intense component with a maximum of 530.9 eV (see Figure 6, *and*). Such bond energy of O1*s* electrons indicates the presence of gallium oxides , according to the data from Ref. [27,28]. Analysis of Ga2$p_{3/2}$ spectrum from the same region (see Figure 7, *a*) confirms the presence of the higher oxide Ga_2O_3, since it contains a single line (1118.5 eV) corresponding to gallium atoms in the state Ga^{3+}. In addition to the above line, lines with energies of ~ 532 and 533 eV are visible in the spectrum of O1*s*, which represent C–O and O–H bonds, respectively, corresponding to the background hydrocarbon contamination of the surface (see Figure 6, *a*).

It is easy to see that the O1*s* peak in all cases consists of four lines on the spectra obtained from regions irradiated with molecular and atomic ions. Ga–O bond component remains the most intense at 530.9 eV. The relative intensities of ~ 532 and 533 eV lines increase, indicating an increase of the proportion of bonds of oxygen atoms with carbon and hydrogen. Such bonds can be formed as a result of rearrangement of the remaining hydrocarbon contaminants on the surface under the impact of the ion irradiation [30]. A decrease of O1*s* signal intensity was also observed during the irradiation. Since the considered peak reflects the amount of oxygen forming bonds with gallium, its relative content in the near-surface layer of the sample was

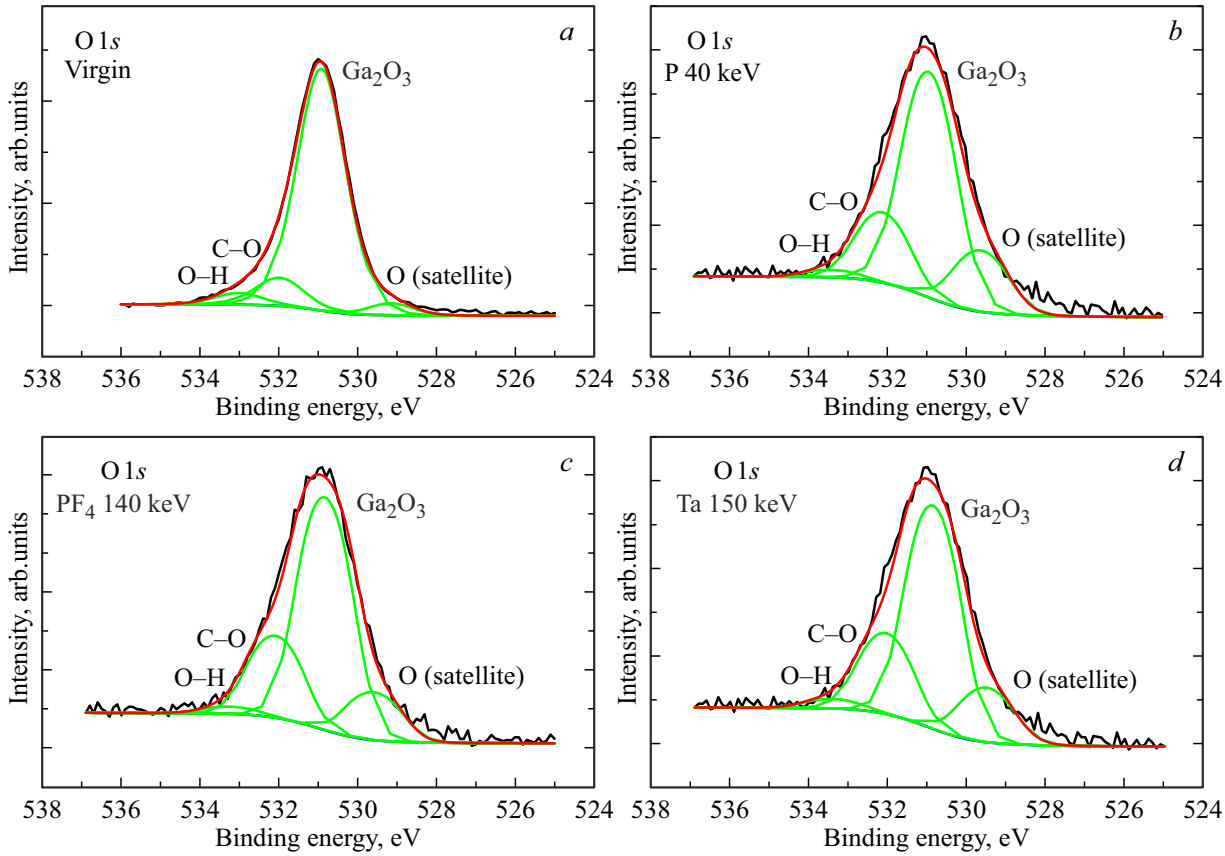

Figure 6. XPS spectra of O1s line of the initial region (*a*) and areas irradiated with a dose of up to 45 dpa of P (*b*), PF_4 (*c*) and Ta ions (*d*).

estimated before and after bombardment and the results of this estimation are listed in Table 4. It is clearly seen that the composition of the thin disordered layer loses a significant part of oxygen during irradiation, while the effect is more pronounced for heavy and molecular ions.

The evolution of the Ga2$p_{3/2}$ spectra after irradiation of Ga_2O_3 target surface with various ions is shown in Figure 7. Decomposition analysis shows that three more components with maxima at 1116, 1117.5, and 1120 eV are added to the main gallium line with a bond energy of 1118.5 eV corresponding to the state Ga^{3+} as a result of ion irradiation. The first two arise from gallium atoms with oxidation degrees of „+“ and „0“. Their appearance can be explained as follows. When accelerated ions are decelerated, in addition to the displacement of atoms from their equilibrium positions in the lattice, significant excitation of the electronic subsystem also occurs, which contributes to the complete (up to the state of Ga^0) or partial (up to the state of Ga^{1+}) reduction of gallium ions. In addition, the chemical state of Ga^{1+} is less thermodynamically stable than Ga^{3+}. For this reason, the lower degree of oxidation in the self-oxidative reduction reaction forms Ga^0 and the more stable ion of Ga^{3+} [30]. It is likely that some of the oxygen atoms can form O_2 molecules, which leave the thin disordered layer, resulting in the above-described decrease in its average concentration (composition decomposition) at least to the depth of XPS analysis (~ 8 nm). Ion bombardment also results in the appearance of another decomposition component in the region of higher energies of 1120 eV. According to the literature data [25,30], this peak may correspond to the so-called shake satellite. The nature of its appearance is based on electron-electron interactions in the system under consideration. The emission of one electron during photoexcitation can result in the excitations in the rest of the electronic subsystem. These excitations require energy, therefore, particles with lower kinetic energy (higher binding energy) appear in the PE spectrum than those corresponding to the ground state of the system after the PE process. This means that the PE spectrum should consist of a main line (representing the ground state after photoexcitation) and an additional line, designated as a satellite, representing the excited states. The stability of the position of the components of the main peak in terms of the bond energy indicates that changes in the electronic properties of the surface occur in approximately the same way during irradiation with various ions. And it is the redistribution of electrons around gallium atoms during the formation of an amorphous structure that does not depend on the ion type [31].

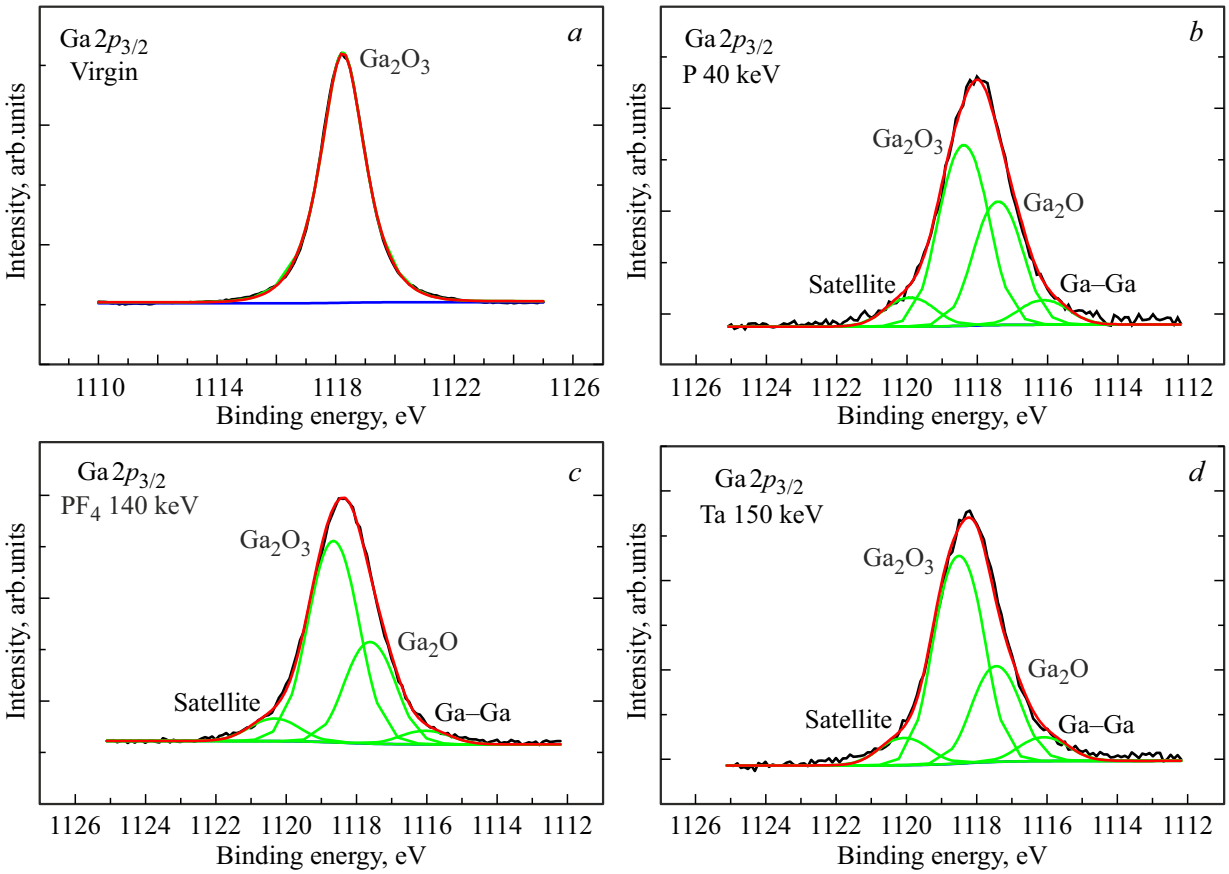

Figure 7. XPS spectra of Ga2$p_{3/2}$ line of the initial region (*a*) and regions irradiated to a dose of 45 dpa by P (*b*), PF_4 (*c*) and Ta ions (*d*).

4. Analysis of the results

Ion bombardment of α-Ga_2O_3 surface does not significantly change the topography. Based on the results of atomic force microscopy, it has already been discussed that the clarity and detail of the small-scale characteristics of the surface relief is lost, but the outlines of the crystallites with which the film grows remain clearly visible. The average roughness values turned out to be approximately the same for the initial and irradiated regions. Also, no significant change of the thickness of the near-surface layer was observed for the high-dose irradiation used in our case. The observed phenomenon is most likely caused by the competition of two processes. Firstly, a swelling (increase of thickness) of the irradiated layer is possible, which is caused by the destruction of the ordered arrangement of atoms in the crystal lattice and the associated increase in the volume of the irradiated layer. Secondly, ion sputtering should occur, accompanying ion bombardment, as a result of which part of the material is removed from the surface and its thickness decreases. In addition, an interruption of the stoichiometric structure of the surface layer (decomposition) occurs at high doses of ions due to the departure of part of the oxygen atoms. The thickness of the modified layer may decrease as a result. Based on the results of RBS/C shown in Figure 5, it can be seen that the accumulation of damage in the target results in the formation of a completely amorphous layer from the target surface.

5. Conclusion

The effects of atomic and molecular ion irradiation on the modification of the surface of a α-Ga_2O_3 material are studied in this paper. The ion irradiation with a dose of up to 45 dpa did not cause any noticeable change in the thickness of the surface layer according to atomic force microscopy data. The clarity and detail of the small-scale characteristics of the surface relief is lost, but the outlines of the crystallites that grow the film remain clearly visible. The average roughness values turned out to be approximately the same for the initial and irradiated regions (0.7 and 0.5 nm, respectively). The RBS results also showed that the accumulation of radiation damage in the target caused the formation of a completely amorphous layer from the surface and into the interior. It was found that P and Ta atomic ions form a thicker amorphous layer at high doses and cause stronger swelling than PF_4 molecular ions. The probable cause of the observed effect is the competition of

two processes: swelling due to the disordering of the crystal structure and a decrease of layer thickness due to sputtering and decomposition. The study of compositio of the disordered layershowed partial change of the oxidation state of Ga atoms up to complete reduction under irradiation with atomic and molecular ions to doses considered. Change of stoichiometry of the near-surface layer (decomposition) due to the partial oxygen loss was also found.

Funding

This study was supported by grant No. 22-19-00166 from the Russian Science Foundation.

Conflict of interest

The authors declare that they have no conflict of interest.

References

[1] S.I. Stepanov, V.I. Nikolaev, V.E. Bougrov, A.E. Romanov. Rev. Adv. Mater. Sci., **44**, 63 (2016).
[2] S.J. Pearton, F. Ren, M. Mastro. *Gallium Oxide, Technology, Devices and Applications* (Elsevier, 2019).
[3] S.J. Pearton, F. Ren, M. Tadjer, J. Kim. Appl. Phys., **9**, 124 (2018).
[4] R. Roy, V.G. Hill, E.F. Osborn. J. Am. Chem. Soc., **74**, 719 (1952).
[5] Feng Shi, Hengyang Qiao. Nano Select., **3**, 348 (2022).
[6] K. Nordlund, M. Ghaly, R. S. Averback, M. Caturla, T. Diaz de la Rubia, J. Tarus. Phys. Rev. B, **57**, 7556 (1998).
[7] A.Yu. Azarov, S.O. Kucheyev, A.I. Titov, P.A. Karaseov. J. Appl. Phys., **35**, 102 (2007).
[8] A.I. Titov, P.A. Karaseov, V.S. Belyakov, K.V. Karabeshkin, A.V. Arkhipov, S.O. Kucheyev, A. Azarov. Vacuum, **315**, 257 (2012).
[9] P.A. Karaseov, K.V. Karabeshkin, A.I. Struchkov, A.I. Pechnikov, V.I. Nikolaev, V.D. Andreeva and A.I.Titov. Semiconductors, **57**, 459 (2023).
[10] A. Azarov, V. Venkatachalapathy, P. Karaseov, A. Titov, K. Karabeshkin, A. Struchkov, A. Kuznetsov. Sci. Rep., **12**, 15366 (2022).
[11] A. Azarov, J.-H. Park, D.-W. Jeon, A. Kuznetsov. Appl. Phys. Lett., **122**, 182104 (2023).
[12] A.I. Titov, K.V. Karabeshkin, A.I. Struchkov, V.I. Nikolaev, A. Azarov, D.S. Gogova, P.A. Karaseov. Vacuum, **200**, 111005 (2022).
[13] A. Finzel, J.W. Gerlach, J. Lorbeer, F. Frost, B. Rauschenbach. Appl. Surf. Sci., **317**, 811 (2014).
[14] S.O. Kucheyev, J.S. Williams, J. Zou, C. Jagadish, G. Li. Appl. Phys. Lett., **77**, 3577 (2000).
[15] A.M. Spool, L. Finney. J. Vac. Sci. Technol. A, **42** (4), 043204 (2024).
[16] R. Huang, F. Li, T. Liu, Y. Zhao, Y. Zhu, Y. Shen, X. Lu, Z. Huang, J. Liu, L. Zhang, S. Zhang, Z. Li, A. Dingsun, H. Yang. Sci. Rep., **8**, 8521 (2018).
[17] Z. Ding, Y.Tang, V. S.K.Chakravadhanula, Q. Ma, F. Tietz, Y. Dai, T. Scherer, C. Kübel. Microscopy, **72**, 326 (2023).
[18] A. Nikolskaya, E. Okulich, D. Korolev, A. Stepanov, D. Nikolichev, A. Mikhaylov, D. Tetelbaum, A. Almaev, C.A. Bolzan, A. Buaczik, R. Giulian, P.L. Grande, A. Kumar, M. Kumar, D. Gogova. J. Vac. Sci. Technol. A, **39**, 030802 (2021).
[19] A.I. Pechnikov, S.I. Stepanov, A.V. Chikiriaka, M.V. Shcheglov, M.A. Odnoblyudov, V.I. Nikolaev. Semiconductors, **53**, 780 (2019).
[20] P.A. Karaseov, A.Yu. Azarov, A.I. Titov, S.O. Kucheev. Semiconductors, **43**, 691 (2009).
[21] J.F. Ziegler, J.P. Biersack, U. Littmark. *The Stopping and Range of Ions in Solids* (Pergamon Press, N.Y., 1985). SRIM-2013 software package available at http://www.srim.org
[22] M. Oda, R. Tokuda, H.Kambara, T. Tanikawa, T. Sasaki, T. Hitora. Appl. Phys. Express, **9**, 021101 (2016).
[23] M. Lee, M. Yang, H.-Y. Lee, H. Uk Lee, H. Lee, H. Son, U.J. Kim. Mater. Sci. Semicond. Proc., **123**, 105565 (2021).
[24] T.-Sh. Chou, A. Akhtar, S.B. Anooz, J. Rehm, O. Ernst, P. Seyidov, A. Fiedler, W. Miller, Z. Galazka, T. Remmele, M. Albrecht, A. Popp. Appl. Surf. Sci., **660**, 159996 (2024).
[25] D. Tamba, O. Kubo, M. Oda, Sh. Osaka, K. Takahashi, H. Tabata, K. Kaneko, Sh. Fujita, M. Katayama. Appl. Surf. Lett., **108**, 251602 (2016).
[26] Y. Xu, C. Zhang, Y. Cheng, Z.-L., Y. Cheng, Q. Feng, D. Chen, J. Zhang, Y. Hao. Materials, **12**, 3670 (2019).
[27] J. Moulder, W. Stickle, W. Sobol, K.D. Bomben. *Handbook of X-Ray Photoelectron Spectroscopy* (Perkin-Elmer Corp., Physical Electronics Division, Eden Prairie, Minnesota, USA, 1992).
[28] A. Mahmoodinezhad, C. Janowitz, F. Naumann, P. Plate, H. Gargouri, K. Henkel, D. Schmeißez, J. Flege. J. Vac. Sci. Technol. A, **3**8, 022404 (2020).
[29] J.E.N. Swallow, J.B. Varley, L.A.H. Jones, J.T. Gibbon, T.D. Vea. APL Materials, **7**, 022528 (2019).
[30] C.L. Hinkle, M. Milojevic, A.M. Sonnet, H.C. Kim, J. Kim, E.M. Vogel, R.M. Wallace. ECS Transactions, **19**, 387 (2009).
[31] S. Hüfner. *Photoelectron Spectroscopy, Photoelectron spectroscopy* (Germany, Berlin, 1995).

Translated by A.Akhtyamov